



RESEARCH LETTER

10.1002/2016GL069918

Key Points:

- Large water vapor mixing ratios (>10 ppmv) were observed in the stratosphere days after the 2015 Calbuco eruption
- The enhancement only lasted for a few days as the mass of water vapor reaching the stratosphere was small (2 Mt)
- The short-lived, small-scale increase resembles those observed after the Kasatochi and Mount St. Helens eruptions

Supporting Information:

- Supporting Information S1
- Movie S1

Correspondence to:

C. E. Sioris,
christopher.sioris@canada.ca

Citation:

Sioris, C. E., A. Malo, C. A. McLinden, and R. D'Amours (2016), Direct injection of water vapor into the stratosphere by volcanic eruptions, *Geophys. Res. Lett.*, *43*, 7694–7700, doi:10.1002/2016GL069918.

Received 24 MAR 2016

Accepted 28 JUN 2016

Accepted article online 1 JUL 2016

Published online 16 JUL 2016

Direct injection of water vapor into the stratosphere by volcanic eruptions

Christopher E. Sioris¹, Alain Malo², Chris A. McLinden¹, and Real D'Amours²

¹Environment and Climate Change Canada, Toronto, Ontario, Canada, ²Environment and Climate Change Canada, Dorval, Quebec, Canada

Abstract While theoretical studies show that water vapor (WV) can be directly injected into the stratosphere during a volcanic eruption, few observations of such a phenomenon exist. The Microwave Limb Sounder observed stratospheric injection of WV following the 2015 Calbuco eruption. Lower stratospheric mixing ratios exceeded 10 ppmv for a few days downwind of the injection location. Plume transport is confirmed by back trajectory modeling. Due to the short duration and limited spatial extent of the enhancement, climatic impact is expected to be negligible. This letter provides spatiotemporal analysis of a volcanogenic pulse of lower stratospheric WV as it dispersed. The inferred mass of stratospheric WV from this eruption of 2 megaton (Mt) and the rapid evanescence of the enhancement are similar to what has been observed for other eruptions, suggesting that injection by moderately explosive eruptions is not an effective mechanism for large-scale stratospheric hydration.

1. Introduction

Water vapor is the most dominant trapper of outgoing infrared radiation, accounting for half of the greenhouse effect [Lacis *et al.*, 2010]. Water vapor enhancements in the lower stratosphere are particularly effective for absorbing outgoing longwave radiation [Solomon *et al.*, 2010]. Enhanced stratospheric water vapor was measured in the 4 day old Mount St. Helens plume using a frost point hygrometer [Murcray *et al.*, 1981]. Following this seminal work, decades have followed with little observational evidence of stratospheric water vapor increases resulting from volcanic eruptions, while numerous modeling studies [e.g., Textor *et al.*, 2003] have shown that moderate global-scale stratospheric enhancements are possible, particularly for eruptions at low latitudes where entrained tropospheric humidity can rival the contribution of the magmatic water. Stratospheric Aerosol and Gas Experiment (SAGE) II observed increases of stratospheric water vapor immediately following the Mount Pinatubo eruption on June 1991 [Fueglistaler *et al.*, 2013]. These enhancements persisted in the SAGE II data record beyond the start of the UARS (Upper Atmospheric Research Satellite) mission in late 1991. Unenhanced stratospheric water vapor measurements in late 1991 from two limb sounders on board UARS, namely, Halogen Occultation Experiment [Fueglistaler *et al.*, 2013] and Microwave Limb Sounder (MLS) [Elson *et al.*, 1996], call the SAGE II measurements into question, especially given the difficulty of separating gas and aerosol extinction signatures in the near infrared with filter-based photometers in the presence of extreme concentrations of particulate matter. For many major eruptions over the past 50 years, including Mount Pinatubo, El Chichón (1982), and Cerro Hudson (1991), in situ water vapor observations in the plume in the days following eruptive stratospheric injection are not available in the peer-reviewed literature. According to a model estimate [Pitari and Mancini, 2002], 37.5 megaton (Mt) of water reached the stratosphere due to Pinatubo, with 10 Mt as vapor, and the majority as ice.

Based on the volcanic explosivity index (VEI) [Newhall and Self, 1982], the 1815 eruption of Tambora (VEI = 7) is the only one clearly more explosive than Pinatubo (VEI = 6) over the past two centuries. According to model simulations [Glaze *et al.*, 1997], the mass of water vapor in the stratosphere was doubled by the direct injection of this eruption, at least initially. Specific humidity can decrease during the evolution of the plume as water vapor is consumed by SO₃ in the process of sulfuric acid formation and because of uptake on the resulting particles. Dehydration was demonstrated for the sulfur-rich, major eruption of Toba using model simulations [Bekki *et al.*, 1996]. Based on measurements in the plume of the 2000 Hekla eruption [Simpson *et al.*, 2001], water is also known to reach the stratosphere in the form of ice coatings on volcanic ash. Water in the condensed phase can quickly vaporize in the dry, ambient air before the particles descend below the tropopause.

Recently, *Schwartz et al.* [2013] used observations by MLS on the Aura satellite to show that the 2008 Kasatochi eruption (VEI = 4) injected water vapor into the lower stratosphere at northern midlatitudes. However, this work also reveals that many other volcanic eruptions of comparable explosivity in the 2004–2012 time frame did not lead to significant enhancements at 100 and 83 mb even though the eruption columns reached such atmospheric pressures. Examples include the eruptions of Grímsvötn in 2011 and Manam in January 2005.

The Chilean volcano Calbuco (41.326°S, 72.614°W) erupted on 22 and 23 April 2015, with the eruption column reaching ≥ 15 km during both events [*Romero et al.*, 2016]. This eruption has a VEI of 4 [*Van Eaton et al.*, 2016].

Here MLS/Aura observations starting on 25 April 2015 are used in combination with back trajectory modeling to demonstrate that the eruption column of Calbuco also delivered water vapor directly into the extratropical lower stratosphere.

2. Data and Methods

The Aura satellite was launched in 2004, bearing MLS and other atmospheric composition sensors. Version 4.2 of the MLS/Aura water vapor and relative humidity with respect to ice (RH_i) products is used in this study. Only data with sufficient quality (>1.45), retrieval convergence (<2), and status (0) (https://mls.jpl.nasa.gov/products/h2o_product.php) are retained. The quality criterion is more stringent than recommended by *Lambert et al.* [2007] and *Read et al.* [2007]. For RH_i, data with sufficient temperature convergence (<1.03) and quality (>0.2 for pressures (p) <100 mb) are used (http://mls.jpl.nasa.gov/products/rhi_product.php). Each water vapor and RH_i profile is retrieved on the same pressure grid with adjacent levels at 121, 100, 83, and 68 mb being most relevant for this study. The vertical resolution for both water vapor and RH_i is ~ 3 – 4 km [*Lambert et al.*, 2007; *Read et al.*, 2007]. The across-track swath at a tangent height of 20 km is ~ 8 km based on the half power beam width in the horizontal direction of the radiometer [*Cofield and Stek*, 2006] used for measuring water vapor [*Lambert et al.*, 2007]. The horizontal resolution in the along-track dimension at these pressure levels is ~ 200 km [*Lambert et al.*, 2007; *Read et al.*, 2007] for both data products. MLS observations are well suited for detecting volcanic injection of water vapor into the stratosphere for three reasons: (1) the microwave radiances are insensitive to volcanic aerosols, (2) there is observational coverage at night, and (3) the dense along-track sampling allows for a two-dimensional retrieval [*Livesey and Read*, 2000], which is ideal for the case of a volcanic plume where spatial heterogeneity in water vapor is expected.

Sulfur dioxide imagery from the nadir-viewing Global Ozone Monitoring Experiment-2 (GOME-2) instrument on Metop-B satellite [*Munro et al.*, 2016] is used to estimate the extent of the plume. The SO₂ vertical column density is retrieved assuming a plume height of 15 km [*Rix et al.*, 2012].

The tropopause pressure is based on the lapse rate as defined by the World Meteorological Organization and is obtained from the MLS data product for its observation geolocations and from National Centers for Environmental Prediction (NCEP) reanalysis data (at a temporal frequency of 4 per day) [*Kalnay et al.*, 1996] over Calbuco.

Modeled back trajectories are used to confirm that the MLS-observed enhancements originated from the Calbuco eruption and that the eruption column extended above the tropopause. Hybrid Single Particle Lagrangian Integrated Trajectory Model (HYSPPLIT) [*Stein et al.*, 2015] is used for this purpose with default settings. MLDP0 (Modèle Lagrangien de Dispersion de Particules d'ordre zéro) [*D'Amours et al.*, 2015; *Webley et al.*, 2009] is used to model the dispersion in order to understand the observed water vapor changes. MLDP0 model inputs are provided as supporting information.

3. Results

The MLS data record presented by *Schwartz et al.* [2013] extends to 2012. Since then, there have been only two eruptions with VEI of ≥ 4 : Kelut and Calbuco. The MLS observations of the Kelut plume during the initial 5 days (13–17 February 2014) are all filtered out based on their low quality. By 17 February 2014, water vapor volume mixing ratio (VMR) is <7 ppm throughout the tropics at 68 mb and therefore not significantly different from the background at this volcanically perturbed pressure level.

Contrary to Kelut, the MLS water vapor data within the Calbuco eruption are of usable quality 3 days after eruption. Note that on 23–24 April 2015, there are data quality limitations (<1.45) for profiles showing

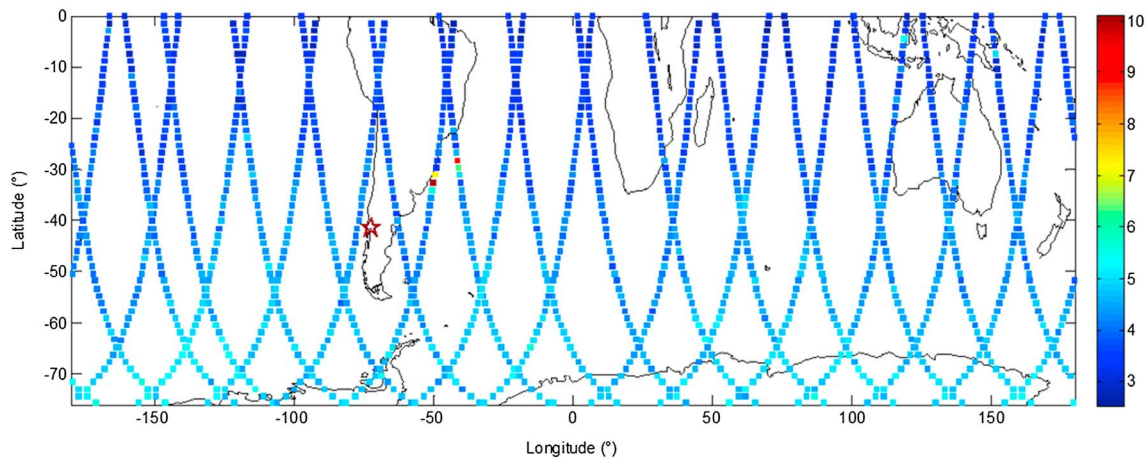


Figure 1. Map of water vapor VMR (ppm) at 68 mb from MLS/Aura observed at two local times, 12 h apart, on 25 April 2015. Middle afternoon sampling runs in a southeast to northwest direction, while nighttime observations run from northeast to southwest. Notice the enhancements off the east coast of South America near 30°S, northeast of the Calbuco volcano (red star). The enhancement on the nighttime overpass (to the west) precedes the daytime orbit.

enhancements in the vicinity of Calbuco and on 22 April 2015, no enhancements are observed in this area. At 32.6°S, 50.1°W on 25 April 2015, MLS observed 10.1 ± 0.4 ppmv at 68 mb (Figures 1 and 2). The high tropopause pressure of 201 mb for this measurement geolocation reflects an extratropical air mass. The pressure level of the enhancement is vertically resolved by MLS from the local tropopause (~18 and ~12 km, respectively).

On 25 April 2015, the largest enhancement is 9 to 10 standard deviations (σ) above the zonal daily mean (ZDM) at each pressure level in the 68–121 mb range for the latitude band extending from the latitude of the eruption (41.3°S) to the northernmost latitude of a global water vapor VMR maximum at these pressure levels within the plume (25.2°S) between 25 and 27 April 2015. On 26 April 2015, the enhancement is 8 to 9 σ above the ZDM VMR (41.3°S–25.2°S) at these pressure levels. By 27 April 2015, the enhancement is vanishing at 68 and 121 mb, while at 83 and 100 mb, the enhancement remains 7 to 8 σ above the ZDM. Finally, by 28 April 2015, at 83 and 100 mb in this zonal band, the water vapor VMR is <5.2 ppm for all observed points and the global maximum VMR for these pressure levels is no longer within this latitude band. The water vapor VMRs at 56 and 146 mb are not significantly enhanced relative to the ZDM at these pressures in the 25–27 April 2015 period.

The back trajectories from the geolocations of the MLS-observed enhancements at 83 and 68 mb originate very close to Calbuco at the time of the first eruption event at ~21:00 on 22 April 2015 [Romero et al., 2016],

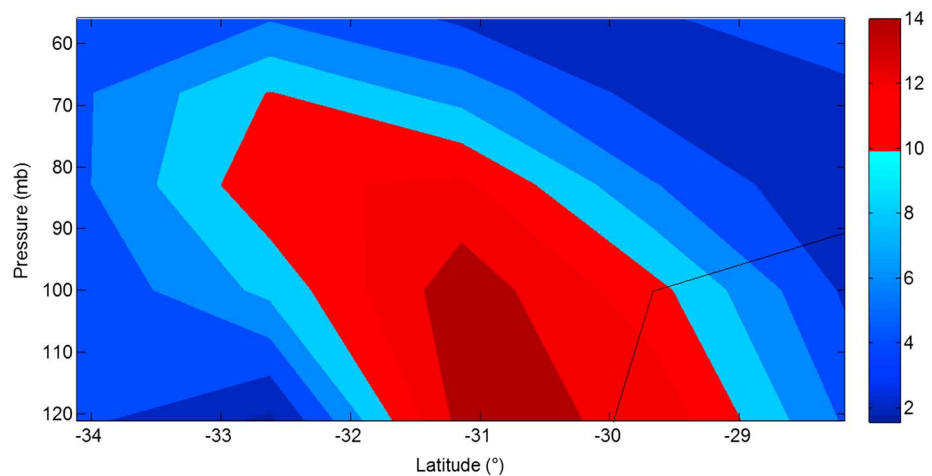


Figure 2. Water vapor VMR (ppm) observed by MLS/Aura in the tropopause region on 25 April 2015 at 04:44 UTC (contains five vertical profiles). The tropopause pressure (black line) is 199 ± 3 hPa for the three profiles south of 30°S in this figure. The longitude for the five scans is $50^\circ\text{W} \pm 0.5^\circ$ and is mapped above (Figure 1).

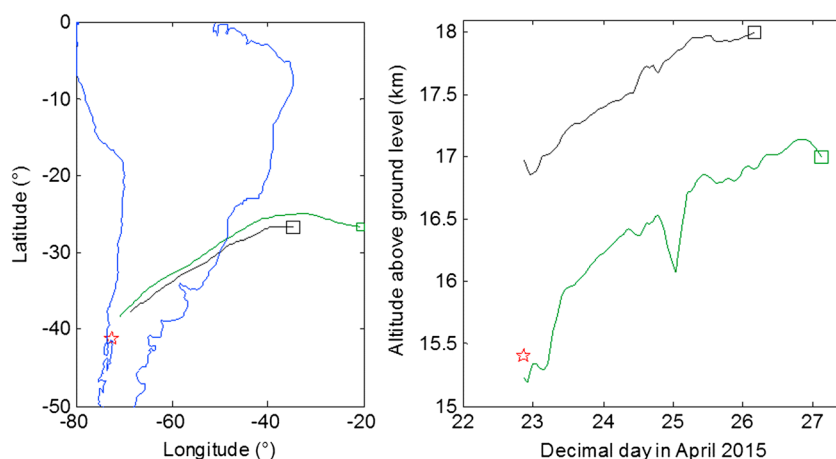


Figure 3. (left) Backward trajectory from the location of the global daily maximum in water vapor VMR observed by MLS on 27 April 2015 at ~03:00 UTC at 83 mb (~17 km, in green) and on 26 April 2015 at ~04:00 UTC at 68 mb (~18 km, in black). A red star indicates the location of Calbuco. (right) Same as Figure 3 (left) but for altitude versus universal time. Squares of matching color indicate the initial geolocations of the backward trajectories. A red star indicates the best estimate of the maximum height of the eruption column and the time of the first eruption event.

with altitudes of 16.6 and 15.7 km, respectively (Figure 3). The tropopause pressure in the NCEP product at the nearest point in space to Calbuco linearly interpolated to the time of the first eruptive event (42.5°S, 72.5°W at 21:00 UTC on 22 April) is 167 mb, which corresponds to a significantly lower height than the plume at that time, indicating that volcanic water vapor was directly injected into the stratosphere in all likelihood. The plume heights at the time of the first eruptive event inferred from HYSPLIT are consistent with the maximum height of the eruption column of 17.4 ± 3.1 km above sea level [Romero *et al.*, 2016]. At 83 mb, the MLS global maximum water vapor VMR on 25 April 2015 of 14.0 ± 0.4 ppm is located at 28.2°S, 41.6°W at ~17:00 UTC. This lies along the 18 km back trajectory in Figure 3, confirming the accuracy of the back trajectory modeling.

4. Discussion and Conclusions

Schwartz *et al.* [2013] found northern midlatitude water vapor VMR in excess of 9 ppmv reaching 83 mb following the 2008 Kasatochi eruption in two independent measurements, implying that these VMRs only lasted for ~1 day. Similarly, the high stratospheric water vapor VMRs due to the eruption of Mount St. Helens had vanished on a subsequent flight 9 days after eruption [Murcray *et al.*, 1981]. In spite of the long lifetime of water vapor in the stratosphere, the MLS-observed enhancements following the 2015 Calbuco (Figure 4) are too small in terms of their spatial scale to remain above the background level for even a week given the plume dispersion (see supporting information). Removal of water vapor by condensation on falling ice could also be involved in the decrease between 25 and 26 April at 83 mb (Figure 4) based on the MLS relative humidity of ~100%, but not at 68 mb as RHi at the latter pressure is too low (<30%). By 26 April 2015, RHi is $(39 \pm 4)\%$ at 83 mb. The presence of volcanogenic ice in the lower stratosphere has been simulated by Van Eaton *et al.* [2016] for 23 April 2016.

The spatial scale of the Mount St. Helens stratospheric water vapor enhancement was also small as indicated by the fact that within the plume, background water vapor VMRs were also sampled [Murcray *et al.*, 1981]. As expected, the Mount St. Helens eruption, by virtue of being a more explosive eruption (VEI = 5), likely delivered more water vapor to the stratosphere, based on the 64 ± 4 ppmv observation [Murcray *et al.*, 1981], although the sampled volume of air for this in situ measurement was of a smaller vertical extent than the MLS vertical resolution by at least a factor of 2. The uncertainty on the Murcray *et al.* [1981] frost point hygrometer measurement has been estimated using a 1 K uncertainty in dew point temperature [Mastenbrook, 1968].

The only previous empirical estimate of the stratospheric mass of water vapor from a volcanic eruption was provided by Murcray *et al.* [1981], who calculated a value of 3.2 Mt for the Mount St. Helens eruption. Encouragingly, this mass agrees with that simulated by Glaze *et al.* [1997] for an eruption with a mass discharge rate and duration similar to the actual values for Mount St. Helens [Carey *et al.*, 1990]. To put this

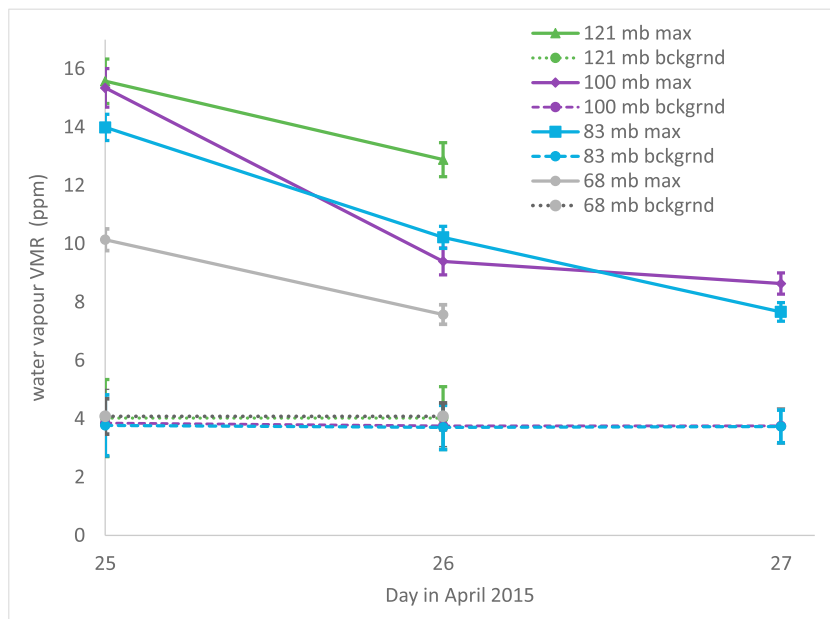


Figure 4. Temporal evolution of the daily global maximum (max) in water vapor VMR at four relevant pressure levels. The global maximum on these days occurs within the Calbuco plume which moves northeast and covers latitude and longitude ranges of 41°S–25°S and 73°W–20°W, respectively, over this period. The zonal (41.3°S–25.2°S) daily mean VMR (bckgrnd) is also shown. The error bar on each global maximum is its measurement precision, while for the ZDM, ±1 standard deviation is shown (with $N \geq 199$ at all four pressures on all days).

mass of water vapor into context, consider that it represents <1% of the 900 Mt/year of water vapor crosses the 385 K isentrope [Yang and Tung, 1996], assuming a local VMR of 3.7 ppmv [Nassar et al., 2005]. Stratospheric methane oxidation delivers 45 Mt/year of water vapor [Lee et al., 2010], so in that context,

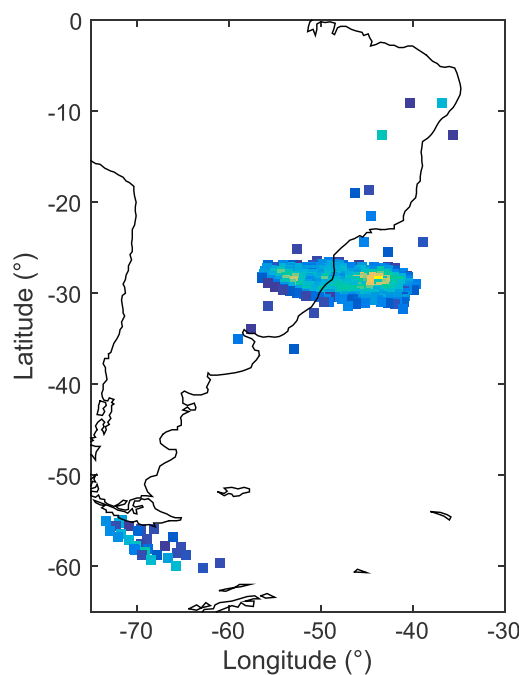


Figure 5. GOME-2/Metop-B SO₂ column density map (DU) for ground pixels with ≥ 7 DU on 25 April 2015 at 1300 UTC. The Calbuco plume is the region of highest SO₂ columns near 30°S, 50°W.

the mass of water vapor from the Mount St. Helens eruption is only 14 times smaller than the annual contribution from this slowly releasing source.

Here the mass of stratospheric water vapor injected by a volcanic eruption is determined using satellite observations for the first time. Limb sounders have the advantage of sampling a given vertical range more rapidly than in situ instruments. The mass of water vapor in the stratosphere 3 days after the Calbuco eruption is inferred from the earliest available MLS orbit to sample the plume (Figures 1 and 2). Tropopause information along the MLS orbit was used to distinguish between upper tropospheric and lower stratospheric air as the mass of water vapor injected into the stratosphere is sought. The longitudinal extent of the plume is estimated to be 16° or 1500 km based on SO₂ column density imagery from GOME-2 (at 13:00 UTC on 25 April 2015, Figure 5). The latitudinal extent of 500 km can be

estimated directly from the MLS observations which are separated by ~ 165 km in latitude at 30°S . The water vapor background is removed as a function of pressure, averaging the VMR from the measurements adjacent to the plume in the north and south directions from the same orbit (see Figure 2). Negative concentration anomalies (relative to the background) at any pressure level of any profile within the plume are set to zero. The Calbuco water vapor mass enhancement of 1.8 Mt is estimated for pressures ≤ 121 mb, of which 1.5 Mt is clearly in the stratosphere. The latter value is half of the mass of stratospheric water vapor injected by Mount St. Helens. The largest sources of uncertainty in the estimated water vapor mass from Calbuco are the longitudinal extent of the water vapor enhancement and the uniformity of the water vapor VMR within the longitudinal extent of the plume. The peak of the water vapor mass enhancement is at 100 mb, although again there is large uncertainty because the across-track swath of MLS [Cofield and Stek, 2006] is significantly narrower than the stratospheric plume. At 83 mb, the Calbuco injection would raise the water vapor VMR in the Southern Hemisphere by 0.01 ppm assuming a background of 4 ppm.

At these stratospheric altitudes, little mixing with the background air is expected on the timescale of a few days [D'Amours *et al.*, 2010]. The absolute decrease in water vapor with time (Figure 4) can be completely explained by stretching of the plume [D'Amours *et al.*, 2010], induced by horizontal wind variations as shown in the animation (supporting information).

Local increases in stratospheric water vapor following three eruptions, namely, Mount St. Helens, Kasatochi, and Calbuco, all appear to have been short-lived, on the order of a week for Mount St. Helens [Murcray *et al.*, 1981] and Calbuco. The derived stratospheric water vapor mass estimates for Mount St. Helens and Calbuco are one to two orders of magnitude smaller than upper tropospheric water vapor mass perturbations by the Cordón Caulle and Eyjafjallajökull eruptions [Sioris *et al.*, 2016]. The total erupted mass from Mount Saint Helens was 870 Mt [Carey *et al.*, 1990]. Assuming 4.6% of this mass is water vapor [Rutherford *et al.*, 1985], this would translate to 40 Mt of water vapor, which exceeds the estimate by Murcray *et al.* [1981] by an order of magnitude. This deficit in the volcanogenic mass of stratospheric water vapor implies that the tropospheric humidity entrained in the eruption column is likely not the dominant source of the enhanced water vapor which reached the stratosphere. A minor contribution from entrained humidity is expected for an eruption with a mass flux $> 1.7 \times 10^7$ kg/s [Glaze *et al.*, 1997] as was the case for Mount Saint Helens (on 18 May 1980) [Carey *et al.*, 1990]. Rapid condensation can remove 80–90% of the water vapor during the rise of the plume through the troposphere depending on the ambient humidity [Glaze *et al.*, 1997]. Thus, rapid condensation can explain most of the observed deficit in stratospheric water vapor mass from the Mount St. Helens eruption.

Estimates of total erupted mass from the 2015 Calbuco eruption are in the 300–740 Mt range [Romero *et al.*, 2016; Reckziegel *et al.*, 2016; Van Eaton *et al.*, 2016]. Conservatively assuming that 1% of the total erupted mass is water vapor [Durant and Rose, 2009], an expected mass of water vapor from Calbuco is therefore in the 3–7 Mt range. Similar to the 1980 Mount St. Helens eruption, the mass inferred from the water vapor observations in the plume underestimates the expected mass. Rapid condensation would be sufficient to explain the modest deficit in the mass of water vapor inferred from the MLS observations if the assumption of a 1% mass fraction for water vapor is valid.

The main implication of this study is that while moderate-sized volcanoes (VEI of 4–5) tend to directly inject material into the stratosphere, the existing direct evidence from several eruptions, with the largest one being that of Mount Saint Helens, now confirms that this is not an effective mechanism for the large-scale hydration of this overlying atmospheric region.

Acknowledgments

There are no real or perceived financial conflicts of interests for any author for the affiliations listed above and any other affiliation. MLS Level 2 data were obtained from <http://mirador.gsfc.nasa.gov/> and GOME-2 SO₂ data were obtained from <ftp://atmos.caf.dlr.de/gome2b/offline/>. NCEP reanalysis data are provided by the NOAA/OAR/ESRL PSD, Boulder, Colorado, USA, from their website at <http://www.esrl.noaa.gov/psd/>.

References

- Bekki, S., J. A. Pyle, W. Zhong, R. Toumi, J. D. Haigh, and D. M. Pyle (1996), The role of microphysical and chemical processes in prolonging the climate forcing of the Toba eruption, *Geophys. Res. Lett.*, *23*, 2669–2672, doi:10.1029/96GL02088.
- Carey, S., H. Sigurdsson, J. E. Gardner, and W. Criswell (1990), Variations in column height and magma discharge during the May 18, 1980 eruption of Mount St. Helens, *J. Volcanol. Geotherm. Res.*, *43*, 99–112.
- Cofield, R. E., and P. C. Stek (2006), Design and field-of-view calibration of 114–660-GHz optics of the Earth observing system microwave limb sounder, *IEEE Trans. Geosci. Remote Sens.*, *44*, 1166–1181.
- D'Amours, R., A. Malo, R. Servranckx, D. Bensimon, S. Trudel, and J.-P. Gauthier-Bilodeau (2010), Application of the atmospheric Lagrangian particle dispersion model MLDPO to the 2008 eruptions of Okmok and Kasatochi volcanoes, *J. Geophys. Res.*, *115*, D00L11, doi:10.1029/2009JD013602.
- D'Amours, R., A. Malo, T. Flesch, J. Wilson, J.-P. Gauthier, and R. Servranckx (2015), The Canadian Meteorological Centre's atmospheric transport and dispersion modelling suite, *Atmos. Ocean*, *53*, 176–199.

- Durant, A. J., and W. I. Rose (2009), Sedimentological constraints on hydrometeor-enhanced particle deposition: 1992 eruptions of Crater Peak, Alaska, *J. Volcanol. Geotherm. Res.*, *186*, 40–59.
- Elson, L. S., W. G. Read, J. W. Waters, P. W. Mote, J. S. Kinnersley, and R. S. Harwood (1996), Space-time variations in water vapor as observed by the UARS Microwave Limb Sounder, *J. Geophys. Res.*, *101*, 9001–9015, doi:10.1029/95JD03653.
- Fueglistaler, S., et al. (2013), The relation between atmospheric humidity and temperature trends for stratospheric water, *J. Geophys. Res. Atmos.*, *118*, 1052–1074, doi:10.1002/jgrd.50157.
- Glaze, L. S., S. M. Baloga, and L. Wilson (1997), Transport of atmospheric water vapor by volcanic eruption columns, *J. Geophys. Res.*, *102*, 6099–6108, doi:10.1029/96JD03125.
- Kalnay, E., et al. (1996), The NCEP/NCAR 40-year reanalysis project, *Bull. Am. Meteorol. Soc.*, *77*, 437–470.
- Lacis, A. A., G. A. Schmidt, D. Rind, and R. A. Ruedy (2010), Atmospheric CO₂: Principal control knob governing Earth's temperature, *Science*, *330*, 356–359.
- Lambert, A., et al. (2007), Validation of the Aura Microwave Limb Sounder middle atmosphere water vapor and nitrous oxide measurements, *J. Geophys. Res.*, *112*, D24536, doi:10.1029/2007JD008724.
- Lee, D. S., et al. (2010), Transport impacts on atmosphere and climate: Aviation, *Atmos. Environ.*, *44*, 4678–4734.
- Livesey, N. J., and W. G. Read (2000), Direct retrieval of line-of-sight atmospheric structure from limb sounding observations, *Geophys. Res. Lett.*, *27*, 891–894, doi:10.1029/1999GL010964.
- Mastenbrook, H. J. (1968), Water vapor distribution in the stratosphere and high troposphere, *J. Atmos. Sci.*, *25*, 299–311.
- Munro, R., et al. (2016), The GOME-2 instrument on the Metop series of satellites: instrument design, calibration, and level 1 data processing—An overview, *Atmos. Meas. Tech.*, *9*, 1279–1301.
- Murcray, D. G., F. J. Murcray, D. B. Barker, and H. J. Mastenbrook (1981), Changes in stratospheric water vapor associated with the Mount St. Helens eruption, *Science*, *211*, 823–824.
- Nassar, R., P. F. Bernath, C. D. Boone, G. L. Manney, S. D. McLeod, C. P. Rinsland, R. Skelton, and K. A. Walker (2005), Stratospheric abundances of water and methane based on ACE-FTS measurements, *Geophys. Res. Lett.*, *32*, L15S04, doi:10.1029/2005GL022383.
- Newhall, C. G., and S. Self (1982), The volcanic explosivity index (VEI): An estimate of explosive magnitude for historical volcanism, *J. Geophys. Res.*, *87*, 1231–1238, doi:10.1029/JC087iC02p01231.
- Pitari, G., and E. Mancini (2002), Short-term climatic impact of the 1991 volcanic eruption of Mt. Pinatubo and effects on atmospheric tracers, *Nat. Hazard. Earth Syst. Sci.*, *2*, 91–108.
- Read, W. G., et al. (2007), Aura Microwave Limb Sounder upper tropospheric and lower stratospheric H₂O and relative humidity with respect to ice validation, *J. Geophys. Res.*, *112*, D24535, doi:10.1029/2007JD008752.
- Reckziegel, F., E. Bustos, L. Mingari, W. Báez, G. Villarosa, A. Folch, E. Collini, J. Viramonte, J. Romero, and S. Osoreo (2016), Forecasting volcanic ash dispersal and coeval resuspension during the April–May 2015 Calbuco eruption, *J. Volcanol. Geotherm. Res.*, *321*, 44–57.
- Rix, M., P. Valks, N. Hao, D. Loyola, H. Schlager, H. Huntrieser, J. Flemming, U. Koehler, U. Schumann, and A. Inness (2012), Volcanic SO₂, BrO and plume height estimations using GOME-2 satellite measurements during the eruption of Eyjafjallajökull in May 2010, *J. Geophys. Res.*, *117*, D00U19, doi:10.1029/2011JD016718.
- Romero, J. E., et al. (2016), Eruption dynamics of the 22–23 April 2015 Calbuco volcano (southern Chile): Analyses of tephra fall deposits, *J. Volcanol. Geotherm. Res.*, *317*, 15–29.
- Rutherford, M. J., H. Sigurdsson, S. Carey, and A. Davis (1985), The May 18, 1980, eruption of Mount St. Helens, 1. Melt composition and experimental phase equilibria, *J. Geophys. Res.*, *90*, 2929–2947, doi:10.1029/JB090iB04p02929.
- Schwartz, M. J., W. G. Read, M. L. Santee, N. J. Livesey, L. Froidevaux, A. Lambert, and G. L. Manney (2013), Convectively injected water vapor in the North American summer lowermost stratosphere, *Geophys. Res. Lett.*, *40*, 2316–2321, doi:10.1002/grl.50421.
- Simpson, J. J., G. L. Hufford, D. Pieri, and J. S. Berg (2001), Response to “Comments on ‘Failures in detecting volcanic ash from a satellite-based technique’”, *Remote Sens. Environ.*, *78*, 347–357.
- Sioris, C. E., J. Zou, C. T. McElroy, C. D. Boone, P. E. Sheese, and P. F. Bernath (2016), Water vapour variability in the high-latitude upper troposphere—Part 2: Impact of volcanic eruptions, *Atmos. Chem. Phys.*, *16*, 2207–2219.
- Solomon, S., K. H. Rosenlof, R. W. Portmann, J. S. Daniel, S. M. Davis, T. J. Sanford, and G.-K. Plattner (2010), Contributions of stratospheric water vapor to decadal changes in the rate of global warming, *Science*, *327*, 1219–1223, doi:10.1126/science.1182488.
- Stein, A. F., R. R. Draxler, G. D. Rolph, B. J. B. Stunder, M. D. Cohen, and F. Ngan (2015), NOAA's HYSPLIT atmospheric transport and dispersion modeling system, *Bull. Am. Meteorol. Soc.*, *96*, 2059–2078, doi:10.1175/BAMS-D-14-00110.1.
- Textor, C., H.-F. Graf, M. Herzog, and J. M. Oberhuber (2003), Injection of gases into the stratosphere by explosive volcanic eruptions, *J. Geophys. Res.*, *108*(D19), 4606, doi:10.1029/2002JD002987.
- Van Eaton, A. R., Á. Amigo, D. Bertin, L. G. Mastin, R. E. Giacosa, J. González, O. Valderrama, K. Fontijn, and S. A. Behnke (2016), Volcanic lightning and plume behavior reveal evolving hazards during the April 2015 eruption of Calbuco volcano, Chile, *Geophys. Res. Lett.*, *43*, 3563–3571, doi:10.1002/2016GL068076.
- Webley, P. W., B. J. B. Stunder, and K. G. Dean (2009), Preliminary sensitivity study of eruption source parameters for operational volcanic ash cloud transport and dispersion models—A case study of the August 1992 eruption of the Crater Peak vent, Mount Spurr, Alaska, *J. Volcanol. Geotherm. Res.*, *186*, 108–119.
- Yang, H., and K. K. Tung (1996), Cross-isentropic stratosphere-troposphere exchange of mass and water vapor, *J. Geophys. Res.*, *101*, 9413–9423, doi:10.1029/96JD00057.